Behavior of HPS Cruciform Columns

P.S. Green[1]

Abstract
With the development of high performance steel for use in the U.S. Navy's Fleet of the Future Program, questions have risen concerning the properties of the specific high performance steels termed HSLA (High Strength Low Alloy). Cruciform stub column members were fabricated to examine the inelastic local buckling behavior of HSLA80 and HSLA100 steels and compare those results to similarly fabricated ASTM A36 steel cruciform specimens. The goal of the research is to determine whether the existing limits on local slenderness can be extended to include steels up to and including a nominal yield stress of 100 ksi.

1. Background
High strength steels first came into existence back in the 1960s (McDermott, 1969) when U.S. Steel began to conduct research on grades of steel beyond what was typically being used in bridge and building construction. It wasn't until the early 1990s that a new class of plate steels started to appear called high performance steels (HPS) due to their chemical composition, material attributes, and overall structural performance. HPS exhibit good weldability, have high fracture toughness making them less susceptible to fatigue cracking, and typically do not need to be pre-heated to prevent non-uniform cooling of the base metal, thus producing less hydrogen cracking. Another attribute of HPS is its high strength; they have a high yield stress allowing them to experience a higher load-carrying capacity. Both HSLA80 and HSLA100 that were tested as part of this research meet these HPS criteria.

Although the characteristics listed add to the HSLA steel's performance, there are some mechanical properties that must be taken into consideration in structural design, especially in high seismic areas. First, these steels have a higher yield to ultimate stress ratio, or yield ratio (YR) when compared to more conventional steels. Though the work is being compared against test specimens fabricated from A36 steel, similar results would be seen if the base comparison would have been ASTM A572 Gr. 50 or ASTM A992 steel. Fig. 1 shows the stress-strain diagrams for both A36 and HSLA80 steels, along with their calculated yield ratios. The second mechanical property that needs to be evaluated is the steel's ductility ratio (DR), or the ratio of ultimate strain to yield strain. Again, for HSLA steels this ratio is smaller than conventional steels. The third mechanical property of HSLA steels that must be considered is the strain-hardening modulus, E_{st}. For HSLA80 steel, its E_{st} value is approximately one-third that of A36

---

[1] Senior Civil Engineer, Bechtel Power Corporation, Frederick, MD, <pgreen2@bechtel.com>

steel. These three properties reduce both the ductility of the material and the inelastic deformation that might occur when structures are constructed with these high performance materials, making them important considerations for design.
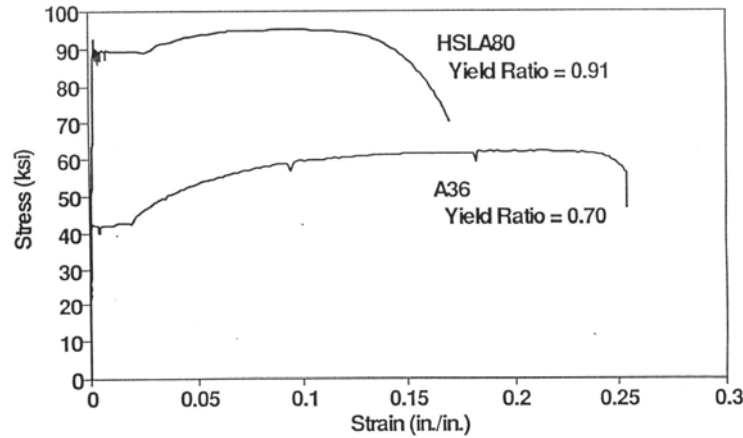

Figure 1: Stress-Strain Curves for Conventional and HPS Steels

One other factor in design is inelastic local buckling. With the decreased ductility of the HSLA steels, members made of these materials must be able to endure this buckling. To do this, the member must fit the criteria for a compact section. The AISC Specifications starting with the First LRFD Edition (AISC, 1986) through the current Fourteenth Edition (AISC, 2010) have had numerous expressions demonstrating whether a compression element is compact, noncompact or slender. Table B5.1, Limiting Width-Thickness Ratios for Compression Elements (AISC, 1986) provided limits for these classifications, though in some instances no limit was provided for a certain classification. The most familiar expression that appears in the table for a compression element is for "Flanges of I-shaped hybrid or welded beams in flexure". This element is said to be compact if it meets or exceeds the following limit:

$$\frac{b}{t} \leq \frac{65}{\sqrt{F_y}} \tag{1}$$

where b is half the full nominal width of the flange. Eq. 1 was originally derived from empirical test data and has since become the "definition" of a compact section.

McDermott (1969) conducted experiments on cruciform columns fabricated from ASTM A514 steel to examine their inelastic local buckling behavior. The shape was selected for its ability to act as four separate flanges when subjected to axial compression. Ideally, the flanges of the specimens were to simultaneously exhibit inelastic local buckling, therefore providing data related to what should be the limiting flange slenderness value (b/t or b/2t, where b is the full width). Since Eq. 1 had not yet been established when McDermott carried out his experiments Eq. 2 was used to determine a limiting value. Therefore, the premise for flanges of plastically designed A514 steel members (F_y =100 ksi) was that the limiting b/t must be less than or equal to 5.1.

$$\frac{b}{t} \leq 8.5 \sqrt{\frac{F_{y\,(A36)}}{F_{y\,(HPS)}}} = \frac{51}{\sqrt{F_y}} = 5.1 \tag{2}$$

The fabrication of the test specimens for McDermott's research consisted of welding two smaller plates of width, b/2 − 0.5t, with a double beveled edge to a larger plate of width b. The weld was a full penetration weld with the fillets ground off flush to the plate. The lengths of the cruciforms, between 3.1b and 3.3b, were chosen so that inelastic local buckling would occur instead of overall column buckling. Once fabricated, the specimens were then stress relieved at 1100º F for one hour. The range of b/2t values were between 2.75 and 10. The specimens were loaded until an average axial compressive strain of 8% was recorded or a well defined buckled shape was observed, whichever came first.

2. Current Study Approach

Previous studies on HSLA80 steel found that this material has a lower ductility than A36 steel and therefore the limiting width-to-thickness ratios established in the code may no longer be valid. A theoretical approach for determining the limiting b/2t (*b/t*) ratio for HPS steel was proposed by Sooi (1993) as,

$$\frac{b}{t} \leq \frac{34}{\sqrt{F_y}} \tag{3}$$

In addition, the AISC LRFD Specification (AISC, 1986) limiting the flange slenderness shown in Eq. 1 had an implied rotational capacity, R, of at least 3 for compact members subject to non-seismic loads.

Table 1 contains the A36, HSLA80 and HSLA100 steel specimen designations and whether they meet the compactness limits established based on Eqs. 1, 2, and 3. These compactness limits are based on nominal material properties and geometries so the *b/t* ratio closest to the limit is listed as "Maybe." Therefore, the nominal b/2t values selected for the test specimens were 3, 6, and 9. The A36 steel specimens represented the control group for the comparisons that will be made.

Table 1: Test Matrix-Nominal Dimensions, Material Properties and Compactness

Steel	Specimen ID	h (Nominal) in.	b (Nominal) in.	F_y (Nominal) ksi	$\frac{b}{t} \leq \frac{65}{\sqrt{F_y}}$	$\frac{b}{t} \leq \frac{51}{\sqrt{F_y}}$	$\frac{b}{t} \leq \frac{34}{\sqrt{F_y}}$
A36	A-3	9	3	36	Yes	Yes	Yes
HSLA80	B-3	9	3	80	Yes	Yes	Yes
HSLA100	C-3	9	3	100	Yes	Yes	Yes
A36	A-6	18	6	36	Yes	Yes	Maybe
HSLA80	B-6	18	6	80	Yes	Maybe	No
HSLA100	C-6	18	6	100	Maybe	No	No
A36	A-9	27	9	36	Yes	Yes	No
HSLA80	B-9	27	9	80	No	No	No
HSLA100	C-9	27	9	100	No	No	No

Experimental testing of cruciform columns composed of HSLA80 and HSLA100 steels was proposed to investigate the validity of Eq. 1, 2, or 3 as there is very little information in the area of inelastic local buckling for these materials. Test specimen fabrication and subsequent testing broadly followed McDermott's procedure (1969) with a few changes introduced. The HSLA specimens were saw-cut from 1/2 inch plate while the A36 specimens were flame cut from 1/2 inch plate. The individual pieces were welded together using pairs of double fillet welds, 1/4 inch for the A36 specimens and 5/16 inch for the HSLA specimens, in lieu of full penetration

welds as in McDermott's experiments. This was done for expediency in producing the nine test specimens and was assumed at the time not to have a significant effect on the experimental behavior other than reducing the b values and these reductions were noted in the analysis of b/2t.

Table 2 specifies the welding processes and consumables used to fabricate the test specimens (see Figs. 2 and 3). These were selected in order to control the heat input and therefore minimize any geometric imperfections that might have been introduced during the fabrication process. Table 3 provides information on the test specimens after they were fabricated so that strength predictions could be made based on the measured cross-sectional and tested material properties for the A36, HSLA80, and HSLA100 cruciform columns.

Table 2: FCAW Weld Process for Specimen Fabrication

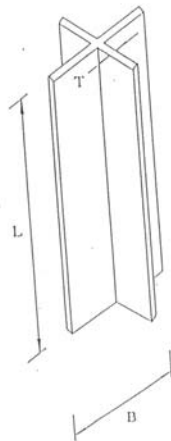| Specimen Type	Nominal Weld Metal Strength, (ksi)	Electrode Designation	Electrode Wire Diameter (in.)	Shielding Gas Composition	Run Speed (cfh)
A	70	ER70s-2	0.030	98% Argon, 2% Oxygen	20
B	90	E91T1K2	0.045	75% Argon, 25% Oxygen	20
C	100	ER100s-1	0.045	98% Argon, 2% Oxygen	20

Figure 2: Typical Specimen Layout

Figure 3: Fabricated Test Specimens

Table 3: Measured and Calculated Test Specimen Properties

Steel	Specimen ID	Tested Yield Stress, ksi	Plate Cross-Sectional Area, in.^{2}	Weld Cross-Sectional Area, in.^{2}	Moment of Inertia, in.^{4}	Radius of Gyration, in.
A36	A-3	48	2.75	0.125	1.154	0.634
HSLA80	B-3	87	5.75	0.195	1.154	0.634
HSLA100	C-3	110	8.75	0.195	1.154	0.634
A36	A-6	48	2.75	0.125	9.065	1.235
HSLA80	B-6	87	5.75	0.195	9.065	1.235
HSLA100	C-6	110	8.75	0.195	9.065	1.235
A36	A-9	48	2.75	0.125	30.471	1.846
HSLA80	B-9	87	5.75	0.195	30.471	1.846
HSLA100	C-9	110	8.75	0.195	30.471	1.846

Unlike the experiments that McDermott carried out, these specimens were not stress relieved, but rather the residual stresses were measured utilizing a Whittemore gage. The device measures a standard 5 or 10 inches to within one ten-thousandth of an inch. Before being used, the gage,

punch bar, and temperature bar were all placed on the steel so they would all be at the same temperature when the measurements were made. Lines were scribed into the plates at specified increments (see Fig.4). The punch bar was then placed on the line and two holes were punched using a hammer. The holes were then drilled using a counter-sink bit. The speed of the drill had to be reduced to prevent the bits from breaking so a voltage control device was attached to the hand drill and set at a 15% voltage reduction. The drill had to be kept completely vertical for both accuracy of the gage and to prevent the drill bit from breaking. The holes were drilled deep enough so that a small 'shoulder' was formed by the counter-sink. This allowed the Whittemore gage pins to rest securely in the holes allowing for accurate readings. Three measurements were taken per hole and an average of the three was reported. Three measurements were taken because of the variance in the Whittemore gage readings. After measuring the plates for each specimen, the pieces were welded together and the measurements were again taken. The difference in the measurements is related to the stresses that developed during the welding process as determined by Eq. 4. To the best of the author's knowledge, this was the first time residual stress measurements were acquired without using the sectioning method or special strain gages whereby the specimens are destroyed during the process of data collection (SSRC 2011).

$$\sigma_{residual} = \frac{l - l_0}{l_0} E \qquad (4)$$

Based on the measured data, idealized residual stress patterns were developed for the A36, HSLA80, and HSLA100 cruciform columns. The measured and idealized residual stress patterns for Specimen B-6 (HSLA80) are presented in Figs. 5 and 6, respectively, as a composite of the four plates that make up the test specimen.

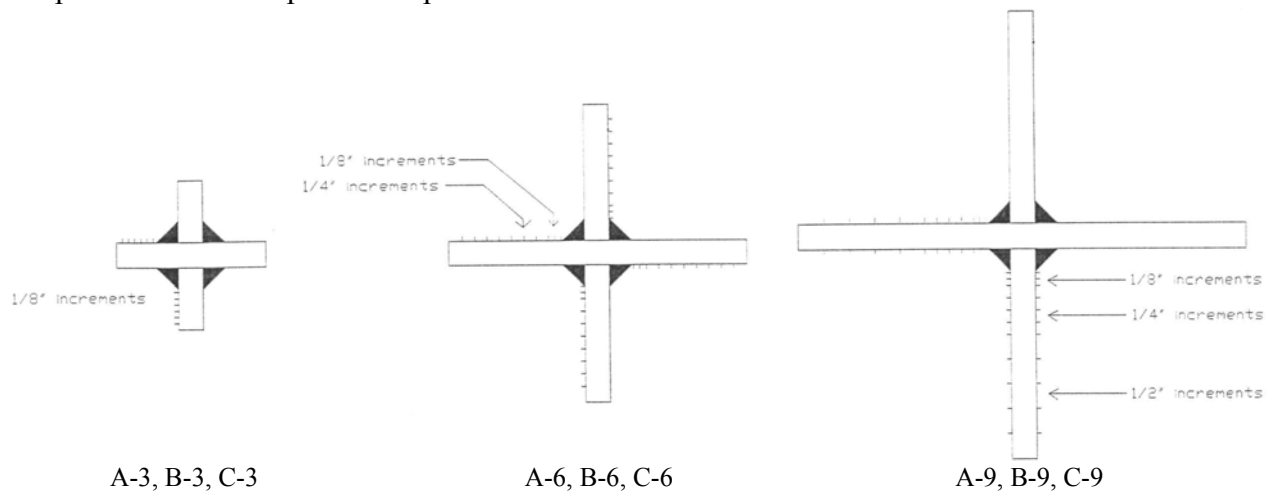A-3, B-3, C-3   A-6, B-6, C-6   A-9, B-9, C-9

Figure 4 Locations Along Plates Where Residual Stresses Were Measured
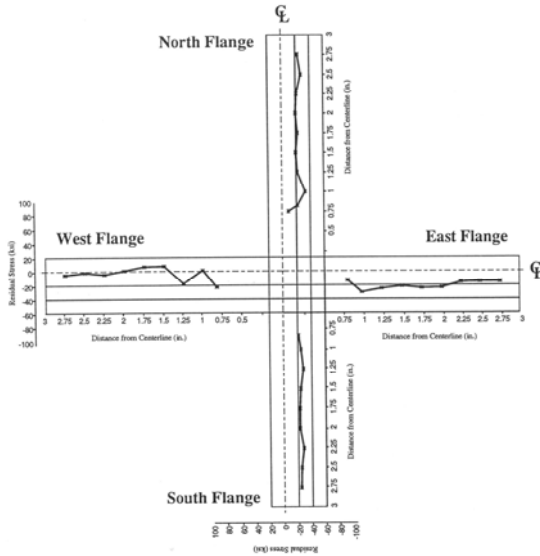
Figure 5 Measured Residual Stress Pattern, Specimen B-6
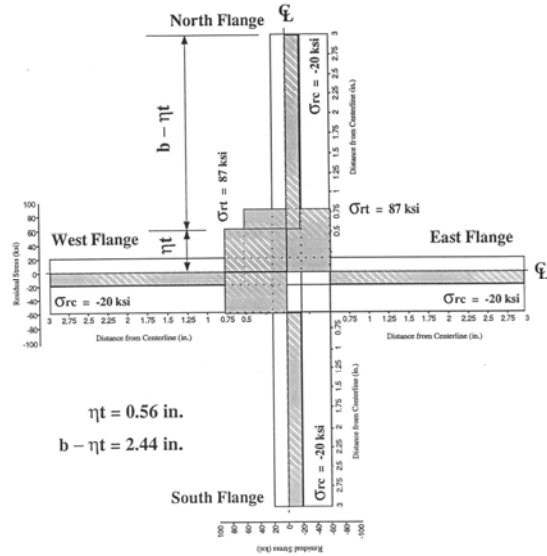

Figure 6 Idealized Residual Stress Pattern for HSLA80 Cruciform Columns

3. Instrumentation and Initial Measurements

3.1 Instrumentation

The following types of instrumentation were placed on each specimen: ten strain gages, four string pots, and four linear variable differential transformers (LVDTs) as depicted in Fig. 7. Two gages labeled "alignment" were used to check that each specimen was correctly placed in the testing machine. If it was not properly placed, at least one flange could have seen a different load than the other flanges. When that occurred, the specimen was adjusted and the alignment gages checked again. The other eight strain gages were placed in pairs on opposite faces of each outstanding flange plate. They would initially show the same strain readings, reflecting that each flange was only being subjected to axial compression. Once a flange started to locally deform out-of-plane, i.e. locally buckle, one gage would show increasing compressive strain while the opposite one would show decreasing strain with increasing axial compression. The LVDTs were used to measure both horizontal and vertical deflections with the horizontal LVDTs aiding in the determination of the onset of plate local buckling while the vertical LVDTs were used to measure the axial shortening of the specimens. The specimens were tested at Lehigh University in Fritz Laboratory's 5000 kip Baldwin Universal Testing Machine.
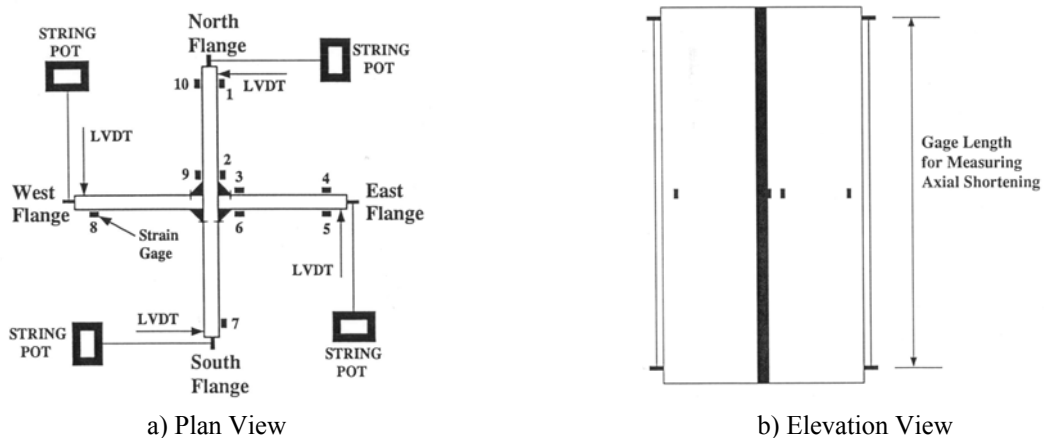

a) Plan View

b) Elevation View

Figure 7: Typical Instrumentation Layout for Cruciform Columns

6

3.2 Initial Measurements

Initial sweep and out-of-flatness measurements were taken for each specimen. The initial sweep measurements consisted of surveying the East – West edges and the North – South edges at a vertical increment of $l/8$ to evaluate whether any of the specimens after fabrication were out of plumb by more than a limiting value. Table 4 gives the maximum sweep measured for each of the 18 in. long specimens (A-6, B-6, and C-6). Similar results were obtained for the 9 in. (A-3, B-3, and C-3) and 27 in. long specimens (A-9, B-9, and C-9). Fig. 8 shows the Sweep Measurements taken for Specimen B-6 along the East – West edges.

Initial out-of-flatness measurements consisted of surveying the North, South, East, and West flange plates at a vertical increment of $l/8$ along the inner and outer edges, i.e. along the plates adjacent to the weld and the free edge. Again, these measurements were taken after fabrication to ensure that each plate making up the specimen was not out-of-flat by more than a limiting value. Table 4 gives the maximum out-of-flatness measured for each of the 18 in. long specimens, i.e. Specimens A-6, B-6, and C-6. Similar results were obtained for the 9 in. (Specimens A-3, B-3, and C-3) and 27 in. (Specimens A-9, B-9, and C-9) long specimens. Fig. 9 shows the Out-Of-Flatness Measurements for Specimen A-6 along the North Flange.

Table 4: Maximum Imperfection Measurements in L = 18 in. Cruciform Column Specimens

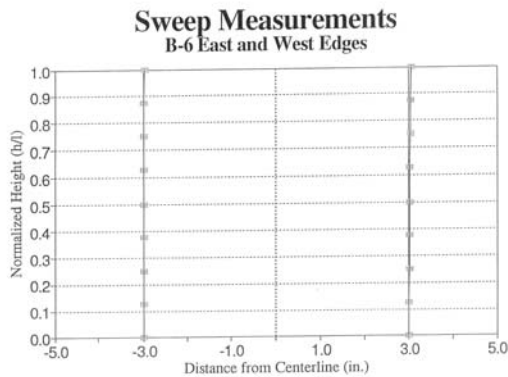| Specimen	Maximum Sweep, δ (in.)	Normalized Sweep δ/L	Maximum Out-of-Flatness, w_o (in.)	Normalized Maximum Out-of-Flatness, $w_o/(b/2)$
A-6	0.065	0.00361	0.049	0.01633
B-6	0.045	0.00250	0.099	0.03300
C-6	0.097	0.00539	0.099	0.03300

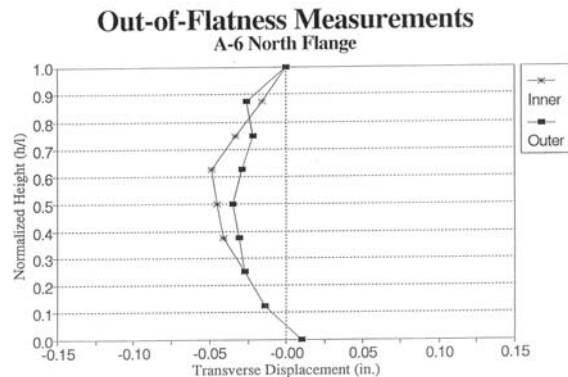Figure 8: Initial Sweep Measurements, Specimen B-6 East and West Edges

Figure 9: Initial Out-of-Flatness Measurements, Specimen A-6 North Flange

4. Experimental Results

Nine cruciform column tests were conducted as previously described in Tables 1, 2, and 3. The columns as designed and fabricated were all considered stub columns as their axial strength and overall behavior was governed by the tested material properties of the plates, measured specimen cross-sectional areas, and the b/2t (*b/t*) ratio of the outstanding flange elements. For each test

specimen, the parameters λ_c, F_{cr}, and P_n are calculated according to the equations presented in Table 5 and their values are given in Table 6 as follows:

- The calculated slenderness parameter, λ_c, was much less than 1.5 or λ_c^2 was much less than 2.25; and
- The calculated critical (buckling) stress, F_{cr}, was essentially equal to the tested material yield stress; and therefore
- The calculated axial compressive strength, P_n, was essentially equal to the yield load, P_y.

Table 5: AISC Specifications Comparison

AISC, 1986		AISC, 2010	
E2. DESIGN COMPRESSIVE STRENGTH	Eq. No.	E3. FLEXURAL BUCKLING OF MEMBERS WITHOUT SLENDER ELEMENTS	Eq. No.
$\lambda_c = \dfrac{Kl}{r\pi}\sqrt{\dfrac{F_y}{E}}$	(E2-4)	$F_e = \dfrac{\pi^2 E}{\left(\dfrac{KL}{r}\right)^2}$	(E3-4)
When $\lambda_c \le 1.5$		When $\dfrac{KL}{r} \le 4.71\sqrt{\dfrac{E}{F_y}}$ $\left(or\ [\lambda_c{}^2] = \dfrac{F_y}{F_e} \le 2.25\right)$	
$F_{cr} = (0.658)^{\lambda_c{}^2} F_y$	(E2-2)	$F_{cr} = \left[0.658^{\frac{F_y}{F_e}}\right] F_y$	(E3-2)
$P_n = A_g F_{cr}$	(E2-1)	$P_n = F_{cr} A_g$	(E3-1)

The axial shortening at the yield load for each test specimen is also provided in Table 6. This information was then used to normalize the test data, e.g. P/P_y or Δ/Δ_y, since the results represent test specimens of similar cross sections and varying material yield strengths.

Table 6: Test Specimen Slenderness, Buckling Stress, Axial Strength, Yield Load, and Axial Shortening at Yield Based on Measured Cross-Sectional and Material Properties

Specimen ID	Slenderness Parameter, λ_c	Critical Buckling Stress, F_{cr}, ksi	Axial Strength, P_n, kips	Yield Load, $P_y = F_y A_g$, kips	Axial Shortening at Yield, $\Delta_y = P_y L/A_g E$, in.
A-3	0.092	47.83	137.5	138	0.0149
B-3	0.124	86.44	248.5	250	0.0267
C-3	0.139	109.11	313.7	316	0.0341
A-6	0.094	47.82	284.3	285	0.0298
B-6	0.127	86.41	513.7	517	0.0540
C-6	0.143	109.06	648.4	654	0.0683
A-9	0.095	47.82	427.7	429	0.0447
B-9	0.128	86.41	772.9	778	0.0810
C-9	0.143	109.06	975.6	984	0.1024

In the current AISC Specification (AISC, 2010) the limiting width-to-thickness ratios are determined based on whether the element being evaluated is subject to axial compression or flexure. Table B4.1a, Width-to-Thickness Ratios: Compression Elements, Members Subject to Axial Compression lists Case 3 for Unstiffened Elements defined as "Legs of single angles, legs of double angles with separators, and all other unstiffened elements." A cruciform column falls

into this case. The limiting *b/t* ratio, λ_r, is calculated to determine whether an element is nonslender or slender as follows:

$$\frac{b}{t} \leq 0.45\sqrt{\frac{E}{F_y}} \tag{5}$$

Using this definition, the limiting *b/t* values for the A36, HSLA80 and HSLA100 specimens are 12.8, 8.6, and 7.7, respectively based on their nominal material yield stress properties.

The final deformed shapes of Specimens A-3, B-3, and C-3 are shown in Figures 10, 11, and 12, respectively. At the extreme axial shortening that these specimens underwent it can be seen that they exhibited both local flange buckling as well as overall global buckling as fixed-fixed columns.

Figure 10: Specimen A-3 Deformed Shape at End of Test
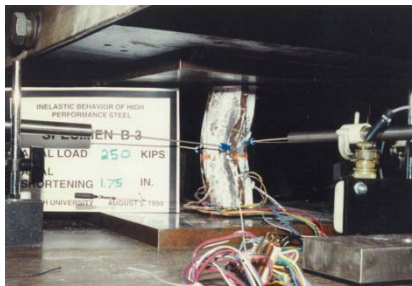
Figure 11: Specimen B-3 Deformed Shape at End of Test

Figure 12: Specimen C-3 Deformed Shape at End of Test

Figures 13, 14, and 15 show Specimens A-6, B-6, and C-6, respectively, at various stages of testing: a) at or near the load corresponding to the onset of one or more of the flange plates moving transversely; b) at or near the maximum load-carrying capacity; and c) the final deformed shape showing local flange buckling of the plates. At the final axial shortening that these specimens underwent, they exhibited only local flange buckling which, when qualitatively evaluated, represents global torsional buckling of the fixed-fixed columns. Specimens A-9, B-9, and C-9 behaved in a very similar manner during experimental testing. The final deformed shape of Specimen A-9 is shown in Fig. 16 looking at the specimen along its length (i.e. elevation view) as well as from above (i.e. plan view).
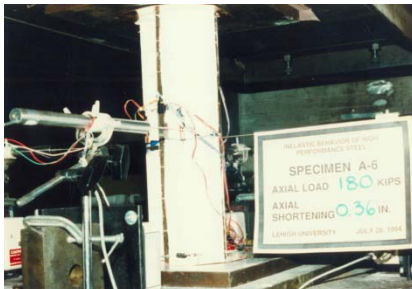
a) Test Specimen Near the Onset of Transverse Plate Movement

b) Test Specimen Near its Maximum Load-carrying Capacity
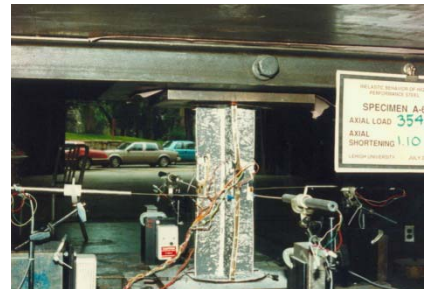
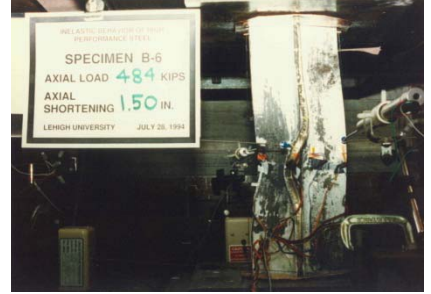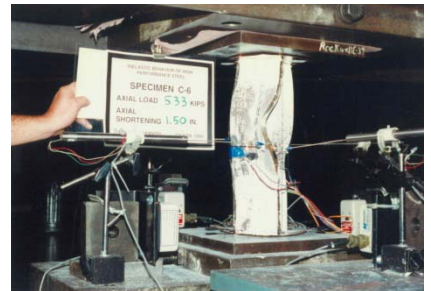c) Test Specimen Deformed Shape at End of Test

Figure 13: Testing of Specimen A-6

9

a) Test Specimen Near the Onset of Transverse Plate Movement

b) Test Specimen Near its Maximum Load-carrying Capacity

c) Test Specimen Deformed Shape at End of Test

Figure 14: Testing of Specimen B-6

a) Test Specimen Near the Onset of Transverse Plate Movement

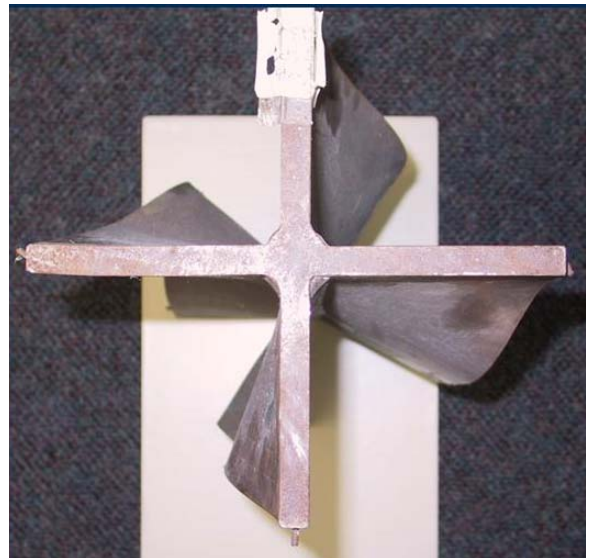b) Test Specimen Near its Maximum Load-carrying Capacity

c) Test Specimen Deformed Shape at End of Test

Figure 15: Testing of Specimen C-6

a)   Inelastic Local Flange Buckling of "Fixed-Fixed" Column, West View, Specimen A-9

b)   Top View, Specimen A-9

Figure 16: Torsional Buckling Due to Inelastic Local Buckling of Four Outstanding Flange Plates, Specimen A-9

5. Discussion

Table 7 provides the maximum axial load and corresponding axial shortening recorded for each test specimen. These values, along with those previously reported in Table 6 were used in evaluating the test results. Figs. 17, 18, and 19 present the test results grouped by their steel yield strengths, i.e. 48, 87, and 110 ksi. Each figure clearly illustrates that for an increasing flange slenderness ratio, b/2t (*b/t*) there is a reduction in the measured axial shortening relative to the overall load-carrying capacity of the specimens from reaching the yield load to a maximum load and subsequently through unloading approaching or passing back through the yield load before the test was concluded. Figs. 20, 21, and 22 present the test results grouped by their flange slenderness ratios, b/2t (*b/t*), i.e. 3, 6, and 9. Each figure clearly illustrates that for an increasing yield strength material there is a reduction in the measured axial shortening relative to the overall load-carrying capacity of the specimens from reaching the yield load to a maximum load and subsequently through unloading approaching or passing back through the yield load before the test was concluded.

Table 7: Test Specimen Results: Maximum Axial Load, P_{max} and Corresponding Axial Shortening, Δ_{max}

Specimen ID	Maximum Axial Load, P_{max} kips	Axial Shortening at Maximum Axial Load, Δ_{max} in.
A-3	227.74	1.044
B-3	297.69	0.657
C-3	362.45	0.678
A-6	353.24	0.831
B-6	595.09	0.572
C-6	697.68	0.414
A-9[1]	409.48	0.241
B-9	832.81	0.281
C-9	1027.97	0.299

(1) Specimen A-9 only achieved a maximum axial load of $0.953P_y$ during the test.
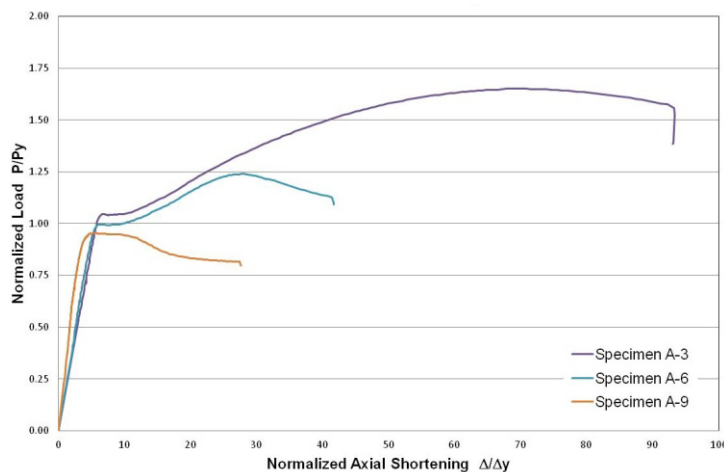

Figure 17: A36 Steel Specimen Results, Normalized Load vs Normalized Axial Shortening
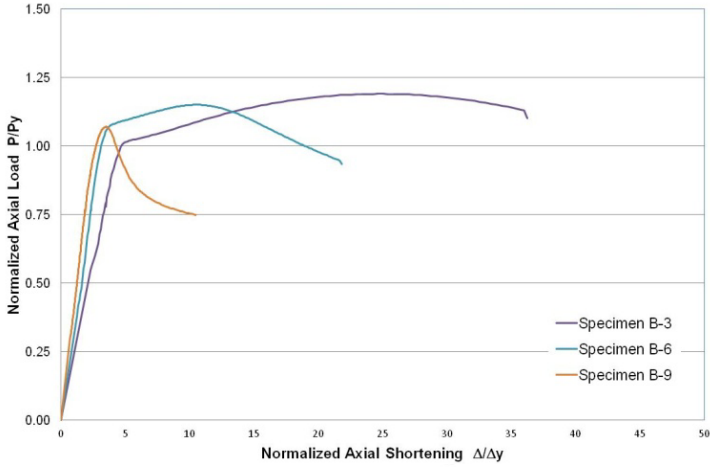
11

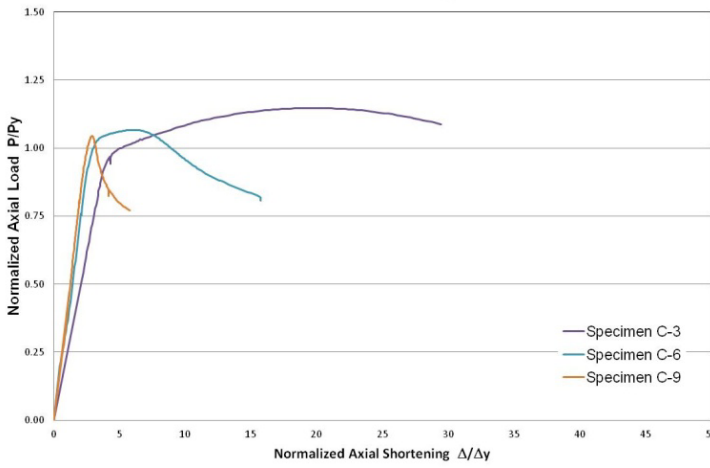Figure 18: HSLA80 Steel Specimen Results, Normalized Load vs Normalized Axial Shortening

Figure 19: HSLA100 Steel Specimen Results, Normalized Load vs Normalized Axial Shortening
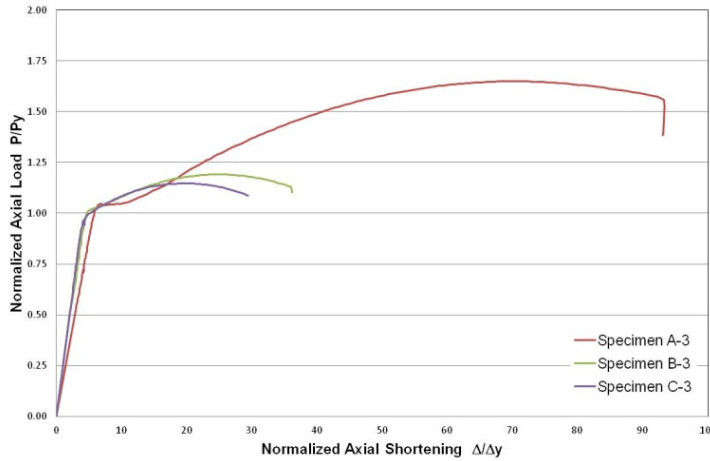

Figure 20: *b/t* = **3** Specimen Results, Normalized Load vs Normalized Axial Shortening
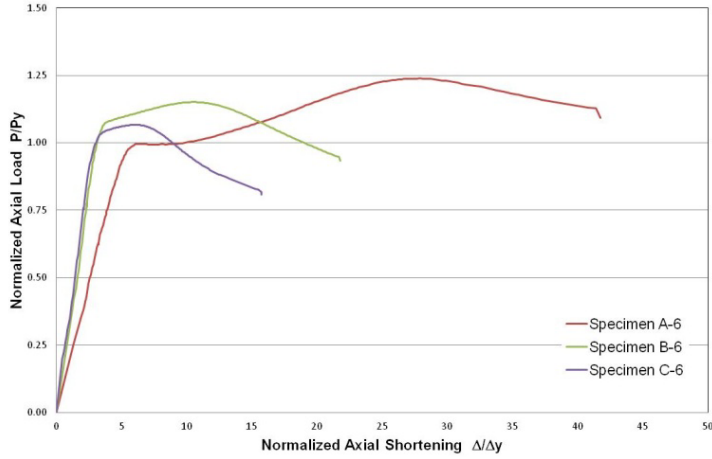
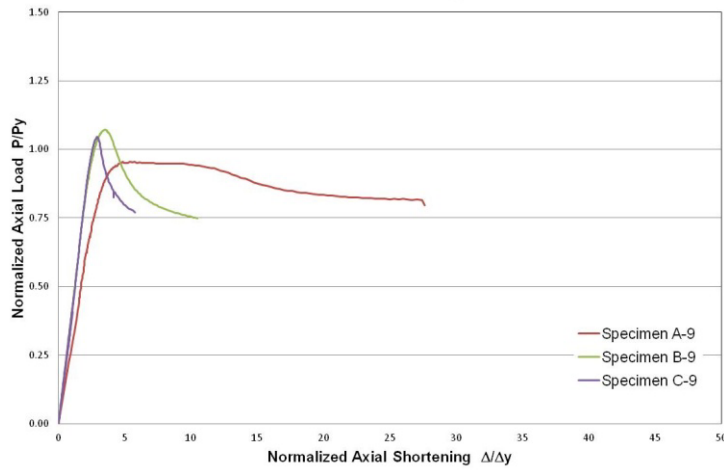Figure 21: *b/t* = **6** Specimen Results, Normalized Load vs Normalized Axial Shortening

Figure 22: *b/t* = **9** Specimen Results, Normalized Load vs Normalized Axial Shortening

The test specimens provided data on the inelastic local buckling of HSLA80 and HSLA100 steels as well as A36 steel. The b/2t (*b/t*) ratios were used to determine the validity of applying the current AISC Specification plate slenderness limits to steels with yield strengths up to and including 100 ksi. Fig. 23 shows the normalized flange slenderness, $\frac{b}{t}\sqrt{F_y}$ versus ductility, R_d curve generated from the data to assess whether the onset of flange local buckling caused the test specimens load-carrying capacity to fall below P_y before a ductility $R_d \geq 3$, was reached. Eq. 6 shows the usual definition for ductility, R which was adjusted in this research as the data was normalized by the calculated value Δ_y given in Table 6 in lieu of using the axial shortening value observed during a test when the calculated value of P_y was first reached.

$$R = \frac{\Delta_u}{\Delta_y} - 1 \tag{6}$$

In Eq. 6 the measured displacement, i.e. axial shortening, when the axial load value again reaches P_y during a test is denoted as Δ_u.

Eq. 7 was used to determine ductility, R_d when the unloading of the specimen after attaining P_{max} did not reach P_y prior to the test being stopped. The measured axial shortening corresponding to the maximum axial load carried by the test specimen is denoted as Δ_{max}.

$$R_d = 2\Delta_{max} - \Delta_y \tag{7}$$

13

Eq. 8 was used to determine ductility, R_d when the unloading of the specimen after attaining P_{max} decreased below P_y before the test was concluded.

$$R_d = \Delta_u - \Delta_y \tag{8}$$

When the ductility ratio is equal to three as shown in Fig. 23 the normalized slenderness is approximately 80. Since the current AISC Specification (AISC, 2010) limits the plate slenderness to 65, both the HSLA80 and HSLA100 steels meet this criterion.
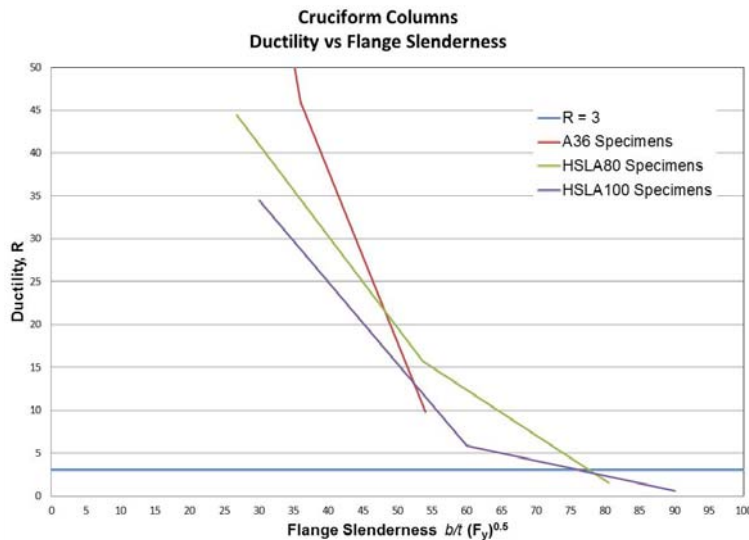

Figure 23: Cruciform Columns, Ductility, R vs Normalized Flange Slenderness

6. Conclusions

The experimental program described in this research study is believed to accurately demonstrate the influence of flange local buckling and material yield strength on the load-carrying capacity of cruciform shaped columns. A series of the test specimens were fabricated having a range of b/2t (*b/t*) ratios from 3 to 9 and steel nominal yield strengths from 36 to 100 ksi. The specimen lengths were held constant with an *l*/b ratio equal to 3 so that the inelastic buckling behavior would not be influenced by overall global buckling. Since it is known that each portion of a cruciform column will act as an individual unstiffened flange, this was also an excellent way to represent one-half of the compression flange of a wide-flange structural member without having it be influenced by any other effects. Also, this methodology has produced reliable results as shown by the research study previously conducted by McDermott (1969).

Based on the experimental data collected on the inelastic flange local buckling behavior of two HPS steels, HSLA80 and HSLA100, the results should be considered a valid representation of other HPS steels whose yield strengths exceed the current material strength limits given in the AISC Specification. Whether the flange width-thickness limit is based on compactness for a flexural member or slenderness for a compression member, this research has shown that the current limits for unstiffened flange elements as described in Table B4.1 (AISC, 2010) are satisfied with steel material yield strengths up to 100 ksi.

References

AISC (1986). "Load and Resistance Factor Design Specification for Structural Steel Buildings." American Institute of Steel Construction, Chicago, IL

AISC (2011). ANSI/N360-11, "Specification for Structural Steel Buildings, June 22, 2010." American Institute of Steel Construction, Chicago, IL

McDermott, J.F. (1969). "Local Plastic Buckling of A514 Steel Members." *ASCE Journal of the Structural Division*, V95, No. ST9 1837-1849.

Sooi, T.K., Ricles, J.M., and Sause, R. (1993). "Proposal to Study Inelastic Behavior of Members and Frames Fabricated from High Performance Steel." Unpublished Proposal. ATLSS Center, Lehigh University, Bethlehem, PA 18015.

Ziemian, R., Editor (2010). **Guide to Stability Design Criteria for Metal Structures**, Sixth Edition, John Wiley & Sons, New York.